Journal of Applied Physics

Energy level alignment and electrical properties of $(Ba, Sr)TiO_3/Al_2O_3$ interfaces for tunable capacitors

Cite as: J. Appl. Phys. **108**, 014113 (2010); https://doi.org/10.1063/1.3459899
Submitted: 02 February 2010 • Accepted: 05 June 2010 • Published Online: 15 July 2010

Shunyi Li, André Wachau, Robert Schafranek, et al.

Energy level alignment and electrical properties of $(Ba,Sr)TiO_3/Al_2O_3$ interfaces for tunable capacitors

Shunyi Li,[1] André Wachau,[1] Robert Schafranek,[1] Andreas Klein,[1,a)] Yuliang Zheng,[2] and Rolf Jakoby[2]
[1]*Materials Science, Technische Universität Darmstadt, Petersenstrasse 32, 64287 Darmstadt, Germany*
[2]*Microwave Engineering, Technische Universität Darmstadt, Merckstrasse 25, 64283 Darmstadt, Germany*

(Received 2 February 2010; accepted 5 June 2010; published online 15 July 2010)

The interface formation between $Ba_{0.6}Sr_{0.4}TiO_3$ and Al_2O_3 has been studied using photoelectron spectroscopy with *in situ* sample preparation. A negligible valence band discontinuity, corresponding to a ~5.6 eV barrier for electron transport at the BST/Al_2O_3 interface is determined. Current-voltage measurements show that the leakage current can be significantly reduced by inserting the Al_2O_3 barrier layer between barium strontium titanate (BST) and Pt electrode. Different charge injection behavior depending on Al_2O_3 thickness is observed, which correspond well with the experimentally determined energy band diagrams. Direct tunneling from the metal electrode into the BST conduction band through the Al_2O_3 barrier layer is observed. © *2010 American Institute of Physics*. [doi:10.1063/1.3459899]

I. INTRODUCTION

Barium strontium titanate (BST) thin films have high tunability of dielectric constant under low tuning voltage. This makes it a promising candidate for tunable integrated components for microwave application such as mobile communications.[1–4] However, one main impediment to this application is the relatively low Schottky barrier between metal electrodes and BST films and therefore a high leakage current.[5] The leakage current is considered as one of the causes for high dielectric loss and short life time under cycling.[6,7] The leakage mechanism is mainly dominated by thermionic emission of charge carriers over the Schottky barrier.[8,9] Insertion of a thin insulating layer in between the metal electrodes and the dielectrics, e.g., SiO_2, could reduce the dielectric loss of BST capacitors.[10] Hence, the contact formation becomes the key issue to understand and improve the electrical properties. The varactors with Pt/BST/Pt structure consist of two back-to-back Schottky barriers and the emission of charge carriers occurs at the barrier under reverse bias.[11] The barrier heights at the top and bottom Pt/BST contact are 0.5 eV and 1.0 eV, respectively, as determined by interface x-ray photoelectron spectroscopy (XPS).[5] A post-growth annealing in O_2 can increase the Schottky barrier height. However, at the top electrode current-voltage (J-V) measurements show generally a higher leakage current which is related to injection from the top contact.[5]

Recent studies have shown that Al_2O_3 can be used as an effective blocking insulator in nonvolatile memory.[12] Al_2O_3 has a wide band gap of 8.8 eV (Ref. 13) and a high resistivity.[14] Besides, Al_2O_3 is thermally and chemically stable at high temperature in oxidizing atmosphere. These properties make Al_2O_3 a good candidate as blocking layer for reduction in charge carrier injection at metal-dielectrics interface of BST varactors.

In this work, the barrier formation at $Ba_{0.6}Sr_{0.4}TiO_3/Al_2O_3$ interfaces is studied using photoelectron spectroscopy. In addition, the leakage current characteristics of BST capacitors with Al_2O_3 barrier layers are reported. Basic structural and dielectric properties of our BST films without Al_2O_3 layer have been reported recently.[15,16] The capacitance and tunability of the films with Al_2O_3 layer can be described using a series capacitor model. Due to the reduced dielectric losses, the overall performance with Al_2O_3 barrier is improved compared to films without Al_2O_3. More details on the dielectric properties will be presented elsewhere. It is noted, however, so far the performance of BST capacitors with Al_2O_3 have not yet reached the same level as the best ones prepared without Al_2O_3 in our laboratory.

II. EXPERIMENTAL

The experiments were performed at the Darmstadt integrated system for materials research, which combines a multitechnique surface analysis system (Physical Electronics PHI 5700) and several deposition chambers by using an ultrahigh vacuum sample transfer.[17] The XPS were recorded with monochromatic Al $K\alpha$ radiation at an emission angle of 45° and a pass energy of 5.85 eV, which gives a total energy resolution of <0.4 eV, as determined from the Gaussian broadening of the Fermi edge of a sputter-cleaned Ag sample. With this resolution, binding energies of core levels and valence band maxima (VBM) can typically be determined with an accuracy of <50 meV and <100 meV, respectively. No charging of the sample was observed during the measurement.

The $Ba_{0.6}Sr_{0.4}TiO_3$ and Al_2O_3 thin films were prepared via rf magnetron sputtering in the same chamber, which has four independent cathodes separated by apertures and a rotatable shutter. BST was first deposited onto $Si(100)/SiO_2/TiO_2/Pt(111)$ substrates from INOSTEK with an rf power density of 2.5 W/cm^2 from a 2 in. ceramic $Ba_{0.6}Sr_{0.4}TiO_3$ target at 650 °C in an Ar/O_2 gas mixture, which contains 1% O_2 at 4 Pa total pressure. After the depo-

a)Electronic mail: aklein@surface.tu-darmstadt.de.

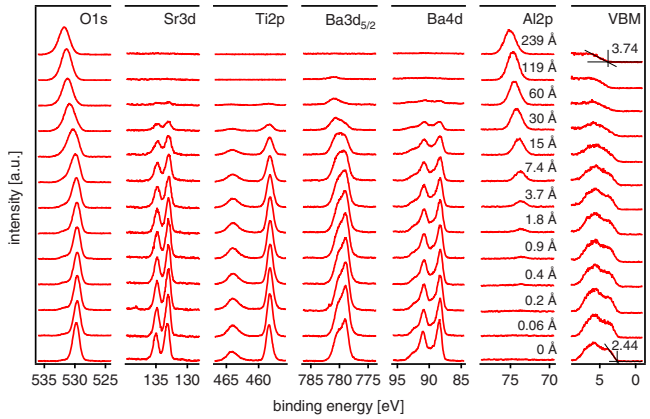

FIG. 1. (Color online) XPS recorded during stepwise deposition of Al_2O_3 onto $Ba_{0.6}Sr_{0.4}TiO_3$. All of the spectra were recorded by using monochromatic Al $K\alpha$ radiation. The Al_2O_3 film thickness indicated is derived from the attenuation of Sr $3d$ and Ti $2p$ core level emission.

sition, the sample was cooled gradually down to room temperature with a rate of 10 K/min in the sputtering atmosphere. Without breaking the vacuum, the Al_2O_3 was deposited onto the BST via reactive sputtering from a 2 in. metallic Al target with rf power density of 2 W/cm^2 using a gas mixture of 95% Ar and 5% O_2 at a total pressure of 0.5 Pa. The Al_2O_3 films are fully oxidized under such conditions as confirmed by XPS. The deposition rate is about 0.5 nm/min as determined by the attenuation of Sr $3d$ and Ti $2p$ photoelectron emission after Al_2O_3 deposition.[18]

For the J-V measurements, samples with parallel-plate structure have been prepared. BST films were first deposited on platinized Si wafer and then covered by Al_2O_3 layer with different thicknesses. Pt electrodes on the top were deposited by dc magnetron sputtering at room temperature using a metallic Pt target of 2 in. diameter, a power of 10 W and Ar gas pressure of 0.5 Pa. The deposition time was set to 20 min, resulting in a Pt film thickness of ~150 nm. A shadow mask with circular holes of 200 μm diameter was mounted in air.

III. RESULTS AND DISCUSSION

A. Deposition of Al_2O_3 on BST

Photoelectron spectra recorded during stepwise deposition of Al_2O_3 onto BST are shown in Fig. 1. 200 nm BST was deposited as substrate layer at the beginning of the experiment by using the deposition conditions described above. As the Al_2O_3 deposition proceeds, the substrate core levels are gradually attenuated and the intensities of Al_2O_3 emissions increase. All substrate emissions decay exponentially with a decay constant corresponding to the inelastic mean free path of the individual emissions, which indicates an abrupt interface formation.[18]

At low coverage of Al_2O_3 the O $1s$ core level has a binding energy of 529.6 eV, showing a narrow and symmetric shape typical for BST.[5] After the Al_2O_3 layer reaches about 7 Å thickness, the peaks start to get broadened and shift to higher binding energy. This is due to the transition from oxygen in BST to that in Al_2O_3. The emissions of Sr $3d$ and Ti $2p$ core levels show both a doublet peak and no obvious change in shape up to 60 Å when they are no longer detectable. Growth of the Al_2O_3 layer is indicated by the steady increase in the Al $2p$ intensity. The peaks of Al $2p$ under low coverage appear at about 73.6 ± 0.1 eV, which corresponds to the binding energy of Al $2p$ in Al_2O_3.[18] This indicates full oxidation of Al during the deposition. They also exhibit a constant peak shape with the deposition going on. The binding energy of Al $2p$ first undergoes a slight decrease till almost 4 Å thickness and the further deposition leads to a reversal shift toward higher binding energy similar to the O $1s$ emission.

The VBM of the BST substrate and Al_2O_3 layer are determined by linear extrapolation of the leading edge of the valence band emission. Those spectra show a clear transition from BST (VBM at 2.44 eV) to Al_2O_3 (VBM at 3.74 eV) too. The emissions of Ba $3d$ and Ba $4d$ show the typical splitting into bulk barium component with lower binding energy and surface barium component with higher binding energy, respectively.[5,19] The surface component of Ba $3d$ has a higher relative intensity than that of Ba $4d$, which is due to the different surface sensitivity of the core levels. The shape and intensity ratio between surface and bulk component of Ba $3d$ and Ba $4d$ emissions do not change up to 4 Å of Al_2O_3 coverage. According to the curve fitting the energy splitting of the Ba $3d_{5/2}$ is around 1.25 eV, while for Ba $4d$ it is around 1.05 eV. After the Al_2O_3 reaches about 7 Å thickness, the relative intensity of surface component and the energy splitting start to increase. This increase in energy difference is especially pronounced for the Ba $4d$ core level. The binding energy shifts and band alignment are discussed together with the reverse interface formation below.

B. Deposition of BST on Al_2O_3

A layer of Al_2O_3 with thickness of 14 nm was first deposited onto a platinized Si wafer and then heated up to 650 °C in the same atmosphere as the BST deposition. After this annealing the XPS spectra show neither Pt emission nor a metal-like Fermi edge at the VBM, which indicates a complete coverage of Pt with Al_2O_3. For the interface formation, the BST films were prepared under the conditions described above. Before each deposition, the sample was heated in the deposition atmosphere for about half an hour in order to reach the desired substrate temperature. After the deposition was finished, the sample was cooled down to room temperature in the same atmosphere and then transferred to the XPS analysis chamber.

The spectra recorded during stepwise deposition of BST onto Al_2O_3 are shown in Fig. 2. The O $1s$ core level show a transformation opposite to that of the reverse interface formation. It starts with a relatively broad oxygen peak coming from Al_2O_3 substrate. The width of the peak gets larger in the transition region due to the increasing intensity of O $1s$ emission from BST. As the BST layer becomes thicker, the O $1s$ emission from Al_2O_3 is further attenuated and the spectra at higher coverage show a narrow shape typical for BST. The spectra of Al $2p$ core level show clearly the attenuation of the signal from the Al_2O_3 substrate. The peak shape remains unchanged at the beginning and intermediate region, while exhibiting a slight broadening for higher BST

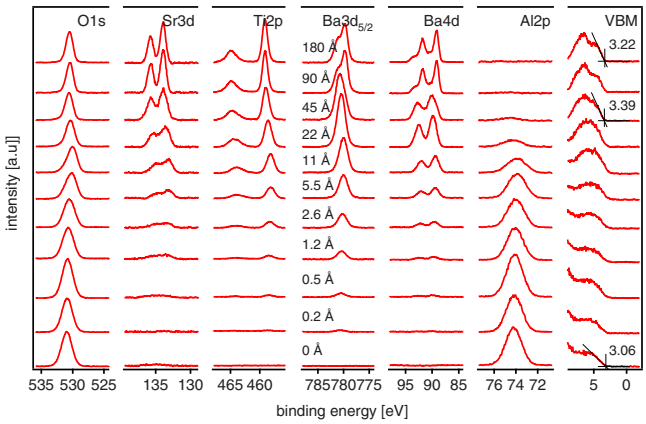

FIG. 2. (Color online) XPS recorded during stepwise deposition of $Ba_{0.6}Sr_{0.4}TiO_3$ onto Al_2O_3. The $Ba_{0.6}Sr_{0.4}TiO_3$ film thickness indicated is derived from the thickness measurement by using ellipsometer.

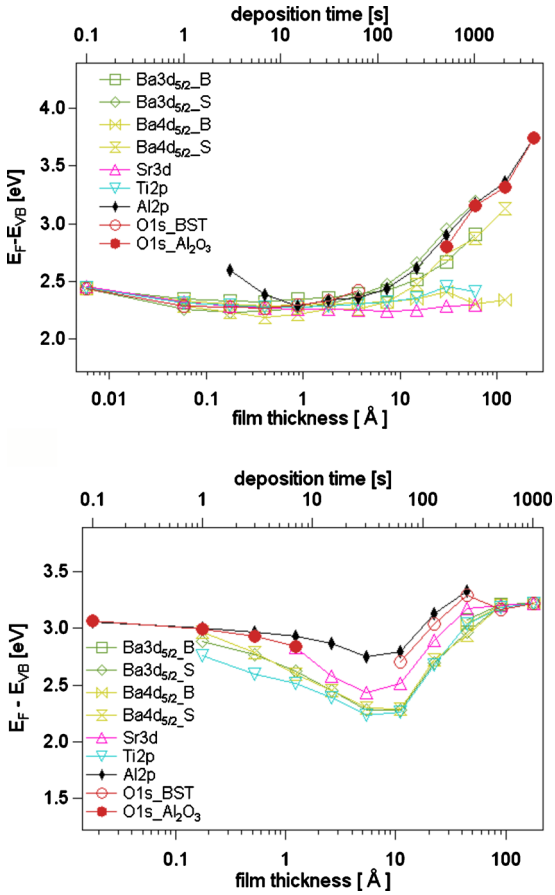

FIG. 3. (Color online) Evolutionary courses of binging energy shifts with increasing film thickness for deposition of Al_2O_3 onto BST (a) BST onto Al_2O_3 (b). (Capital letters B and S represent bulk and surface component, respectively.

thickness. The splitting of the Sr $3d$ doublet is not well resolved until the thickness of BST reaches 45 Å. There is a considerable line broadening at low coverage making the determination of binding energy shifts in the Sr $3d$ core level uncertain. In contrast, the Ti $2p$ doublet has a wider splitting allowing to follow the binding energy shift even at low coverage. In the Ba $3d_{5/2}$ and Ba $4d$ spectra, there is only one component observed for low thickness, before the typical splitting into bulk and surface components starts to appear when the BST layer reaches about 45 Å thickness. A similar behavior is observed during deposition of BST onto Pt.[5] In general, all the peaks from BST become gradually narrower as the film gets thicker. This is mainly because the electronic and crystallographic structure of BST is not fully developed at very low coverage. This may be partially related to the deposition on a dissimilar and probably amorphous substrate. From the initial and final valence band spectrum the values of VBM of Al_2O_3 (3.06 eV) and BST (3.22 eV) are determined, respectively. The evolution of the binding energies are discussed in Sec. III C.

C. Energy level alignment

The evolution of core level binding energies for both interface formations is presented in Fig. 3. For better visibility, the binding energy differences between the core levels and VBM have been subtracted. For the deposition of Al_2O_3 onto BST, as shown in Fig. 3(a), the VBMs of uncovered BST substrate and approximately 240 Å Al_2O_3 top layer correspond to the values determined from the valence band spetra. Same procedure is applied to the deposition of BST onto Al_2O_3, which is shown in Fig. 3(b). The core level to VBM binding energy differences of both experiments are in very good agreement with each other, and also with other experiments.[5,18,20]

In Fig. 3(a) the binding energies of the core levels from BST substrate exhibit almost no shift up to 2 Å. As the thickness of Al_2O_3 increases further, the curves start to separate and different core levels from BST show different binding energy shifts. The Ba $4d$ bulk component, the Sr $3d$ and Ti $2p$ levels show only minor changes in binding energy. However, O $1s$ from BST (taken from O $1s$ spectra when the Al_2O_3 is thinner than 4 Å), together with Ba $3d$ bulk and surface component reveals increasing binding energy shifts. The most pronounced increase in binding energy is observed for the Ba $3d$ surface component. The magnitude of binding energy shift in the BST core levels in Fig. 3(a) follows the ascending order of surface sensitivity. This indicates a strong binding energy shift in only the top atomic layers of BST, as represented by the most surface-sensitive Ba surface components, while the underlying layers, as represented by Sr $3d$, Ti $2p$, and Ba $4d$ bulk component, are not affected.[21] Such a situation may occur in the presence of an electric field in the Al_2O_3 layer, which penetrates the surface of the BST but not the bulk. The electric field is most likely established by charges in the Al_2O_3 layer introduced by the deposition process.[18] The absence of field penetration in the BST bulk requires an interface charge. Such charges are however also indicated by the dielectric properties of the BST/Al_2O_3 capacitors and may explain the increase in intensity ratio of Ba surface and bulk components (see Fig. 1).

For the reverse interface formation, the binding energy shifts in the core levels from BST and those from Al_2O_3 exhibit a parallel evolution in the transition region. The VBM of both substrate and film show first a decrease before the thickness of BST reaches approximately 6 Å. Further deposition leads to an increase in binding energies until the BST layer is about 45 Å thick, where the Ba bulk component

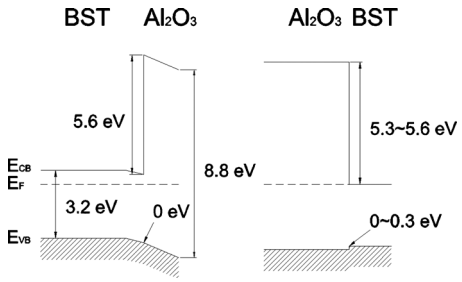

FIG. 4. Energy level alignment of BST/Al_2O_3 (left) and Al_2O_3/BST (right) interfaces. The courses of the bands are extracted after the final deposition step. The band gap energies of BST and Al_2O_3 are taken as 3.2 eV (Ref. 22) and 8.8 eV,[13] respectively.

start to arise in the spectra. The core levels of O 1*s*, Ba 3*d*, Ba 4*d*, Sr 3*d*, and Ti 2*p* all show a saturation of binding energy shifts at this thickness and merge.

The energy level difference of the VBM between Al_2O_3 and BST can be extracted from the difference of the binding energy shifts in the core levels. For the case shown in Fig. 3(a), the VBM derived from Al 2*p* and O 1*s* for Al_2O_3 is very close to the VBM derived from the most surface-sensitive core levels of BST, which indicates a very small valence band discontinuity at the interface. For the reverse case shown by Fig. 3(b), the difference of VBM between BST and Al_2O_3 ranges from 0 eV (if the BST VBM is derived from O 1*s*) to 0.3 eV (for Ba 3*d*, Ba 4*d*, and Ti 2*p*), and in between for Sr 3*d*. An inspection of the valence band spectra shows that the shift in the maximum follows the binding energy evolution of the O 1*s* core level for coverage $\gtrsim$45 Å, where the valence band starts to transform to the typical structure of BST. This indicates that the O 1*s* core level might be the most suitable for the determination of the BST VBM for $\gtrsim$45 Å, which results in a valence band discontinuity of 0 eV. The energy level alignments for both interfaces are shown in Fig. 4. Both interfaces indicate a negligible barrier height in the valence band. This is a reasonable result as the valence bands in both materials are derived from O 2*p* orbitals. A large barrier height is therefore obtained in the conduction band for injection of electrons, due to the large difference in energy gap between Al_2O_3 and BST.

D. J-V measurement

The leakage current measurements were carried out by using a Keithley 2612 source meter. The voltage was stepwise increased (Staircase method) and hold for 1 s before recording each data point. No significant changes have been observed with longer hold times (up to 10 s), indicating that the characteristics is not strongly affected by polarization currents. Compared to the samples studied by Baniecki *et al.*,[23] our samples have much lower capacities due to larger film thickness and additional Al_2O_3 layer, which explains the lower contribution of polarization current in the present study.

For the J-V measurements, three samples have been prepared, using ~250 nm thick $Ba_{0.6}Sr_{0.4}TiO_3$ layers with 0, 2.5, and 10 nm Al_2O_3 layer on top of the BST, respectively. Pt electrodes with a diameter of 200 μm are deposited as

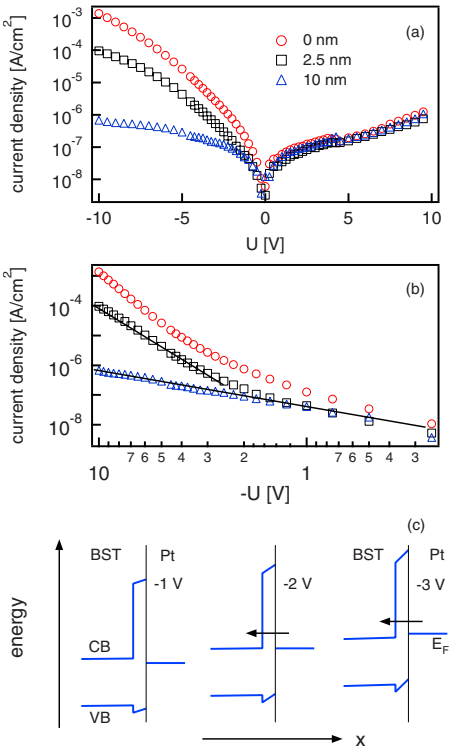

FIG. 5. (Color online) J-V characteristics of $Ba_{0.6}Sr_{0.4}TiO_3$ capacitor with and without Al_2O_3 barrier layer (a). Negative bias voltage corresponds to a reverse bias for the top contact (negative voltage at top). A double logarithmic presentation is of the current for negative bias is shown in (b). The energy band diagram in the vicinity of the Al_2O_3 layer for the sample with 2.5 nm Al_2O_3 with different bias voltages is shown in (c). The arrows indicate direct tunneling through Al_2O_3 from Pt into the BST conduction band.

top contacts. As mentioned above, the Pt/BST/Pt structure has different barrier heights at the top and bottom contacts.[5] This should result in asymmetric J-V curves for the Pt/BST/Pt sample, as demonstrated in Fig. 5.

When the bottom contact is under reverse bias (positive voltage in Fig. 5), the leakage current is provided by electron injection at the bottom Pt/BST contact. In this case, the J-V curves exhibit a field dependence of the barrier height, which is attributed to the Schottky barrier lowering because of the presence of image force.[24]

According to Fig. 5, the current at positive bias voltage is only slightly reduced by Al_2O_3. However, by insertion of the Al_2O_3 layer with its low dielectric constant, the electric field in the BST layer is significantly reduced.[25] Due to the lower electric field in BST, electron injection and the corresponding leakage current is expected to be smaller. The different experimental behavior is probably caused by a low permittivity layer near the bottom contact. Such layers, which are often called *dead layers*, are frequently invoked for ferroelectric materials to explain, e.g., the reduction in permittivity with decreasing thickness (see, e.g., Ref. 26). The presence of a dead layer at the bottom contact would enhance the electric field at the bottom contact and reduce its dependence on the Al_2O_3 thickness.

When the top contact is under reverse bias (negative voltage in Fig. 5), the leakage current of the sample without Al_2O_3 layer is 3 orders of magnitude larger at −10 V than

that of the bottom contact. This is in good agreement with the behavior expected for a smaller barrier height.[5] With the insertion of a thin Al_2O_3 barrier layer in between the BST and Pt top electrode, the leakage current is significantly reduced, especially for the sample with 10 nm Al_2O_3 layer. This result agrees well with the interface experiments, which suggest a large electron barrier height over 5 eV at the BST/Al_2O_3 interface.

The double logarithmic plot of the leakage current for negative voltage [Fig. 5(b)] indicates that at low bias voltage the reduction in leakage current does not depend on Al_2O_3 thickness. In this regime the current depends linearly on voltage, indicating an Ohmic behavior. This is attributed to the leakage of the Al_2O_3 layer, which is prepared at room temperature and thus has an amorphous structure and can be expected to be a less good insulator than crystalline Al_2O_3. The linear dependence of current on voltage is obeyed for all applied voltages of the sample with 10 nm Al_2O_3. Assuming that the leakage current is limited by resistive losses in the Al_2O_3 layer, a resistivity of 10^{13} Ω cm can be derived, which compares well with other reported values.[14]

For voltages $U \leq -2$ V, the slope of the curve increases for the sample with 2.5 nm Al_2O_3. Energy diagrams for 2.5 nm Al_2O_3 at different negative bias voltage are given in Fig. 5(c). It is evident that the Fermi level of the Pt overlaps with the conduction band of the BST. Hence, direct tunneling through the Al_2O_3 layer into empty conduction band states is possible for $U \leq -2$ V. The increased slope of the $j(U)$ curve can therefore be attributed to the onset of electron tunneling. In this regime, the current shows a power law dependence on voltage with an exponent of ~ 4. Both magnitude of current and voltage dependence compare well with calculated tunneling currents of Si metal-oxide-semiconductor-diodes with similar oxide layer thickness.[27] The high-voltage regime is not observed for the sample with 10 nm Al_2O_3. As expected, a 10 nm Al_2O_3 layer is too thick for electron tunneling.

The electron tunneling at the BST/Al_2O_3/Pt contact at low bias voltage becomes possible due to the pronounced potential drop in the Al_2O_3 layer, which is a consequence of its low dielectric constant compared to those of the BST. The Al_2O_3 layer may thus also be regarded as an intentionally inserted *dead layer*, which leads to a significantly larger Schottky barrier lowering effect than for BST.

IV. SUMMARY AND CONCLUSION

We have presented an *in situ* photoemission study of the interface formation of Al_2O_3 and $Ba_{0.6}Sr_{0.4}TiO_3$ prepared via magnetron sputtering. The energy band alignment is characterized by negligible or very small valence band discontinuity. The difference in band gap between Al_2O_3 and BST leads to a large conduction band discontinuity of >5 eV, which provides an effective barrier for electron transport. By insertion of an Al_2O_3 layer at the metal-dielectric interface, the injection of electrons is effectively blocked and a significant reduction in leakage current is observed by J-V measurements. The Al_2O_3 layer also serves as an artificial *dead layer*, which enables direct tunneling into the BST conduction band at low bias voltage for low Al_2O_3 film thickness. The knowledge of the energy band diagram, which is provided by the photoemission experiments, enables a detailed understanding of leakage current mechanisms.

ACKNOWLEDGMENTS

This work was supported by the German Science Foundation in the framework of the research training school GRK 1037 (Tunable Integrated Components for Microwaves and Optics, TICMO).

[1] A. Tagantsev, V. Sherman, K. Astafiev, J. Venkatesh, and N. Setter, J. Electroceram. **11**, 5 (2003).
[2] *Nanoelectronics and Information Technology*, edited by R. Waser (Wiley-VCH, Weinheim, 2003).
[3] P. Bao, T. J. Jackson, X. Wang, and M. J. Lancaster, J. Phys. D: Appl. Phys. **41**, 063001 (2008).
[4] S. Gevorgian, IEEE Microw. Mag. **10**, 93 (2009).
[5] R. Schafranek, S. Payan, M. Maglione, and A. Klein, Phys. Rev. B **77**, 195310 (2008).
[6] S. Yamamichi, A. Yamamichi, D. Park, T. King, and C. Hu, IEEE Trans. Electron Devices **46**, 342 (1999).
[7] S. Huang, H. Chen, S. Wu, and J. Lee, J. Appl. Phys. **84**, 5155 (1998).
[8] G. Dietz, W. Antpoehler, M. Klee, and R. Waser, J. Appl. Phys. **78**, 6113 (1995).
[9] G. Dietz, M. Schumacher, R. Waser, S. Streiffer, C. Basceri, and A. Kingon, J. Appl. Phys. **82**, 2359 (1997).
[10] V. Reymond, D. Michau, S. Payan, and M. Maglione, J. Phys.: Cond. Matter **16**, 9155 (2004).
[11] J. Baniecki, R. Laibowitz, T. Shaw, K. Saenger, P. Duncombe, C. Cabral, D. Kotecki, H. Shen, J. Lian, and Q. Ma, J. Eur. Ceram. Soc. **19**, 1457 (1999).
[12] S. Nakata, S. Nagai, M. Kumeda, T. Kawae, A. Morimoto, and T. Shimizu, J. Vac. Sci. Technol. B **26**, 1373 (2008).
[13] J. Robertson, J. Vac. Sci. Technol. B **18**, 1785 (2000).
[14] M. Voigt and M. Sokolowski, Mater. Sci. Eng., B **109**, 99 (2004).
[15] R. Schafranek, A. Giere, A. G. Balogh, T. Enz, Y. Zheng, P. Scheele, R. Jakoby, and A. Klein, J. Eur. Ceram. Soc. **29**, 1433 (2009).
[16] A. Giere, R. Schafranek, Y. Zheng, H. Maune, M. Sazegar, R. Jakoby, and A. Klein, Frequenz **62**, 52 (2008).
[17] D. Ensling, A. Thissen, Y. Gassenbauer, A. Klein, and W. Jaegermann, Adv. Eng. Mater. **7**, 945 (2005).
[18] Y. Gassenbauer, A. Wachau, and A. Klein, Phys. Chem. Chem. Phys. **11**, 3049 (2009).
[19] J. D. Baniecki, M. Ishii, T. Shioga, K. Kurihara, and S. Miyahara, Appl. Phys. Lett. **89**, 162908 (2006).
[20] R. Schafranek and A. Klein, Solid State Ionics **177**, 1659 (2006).
[21] This does not mean that the surface is composed only of Ba and O. In contrast, we have observed Ba, Sr, and Ti using low energy ion scattering spectroscopy (LEISS), which clearly indicates that all elements are present in the topmost atomic layers.
[22] M. Cardona, Phys. Rev. **140**, A651 (1965).
[23] J. D. Baniecki, T. Shioga, K. Kurihara, and N. Kamehara, J. Appl. Phys. **97**, 114101 (2005).
[24] S. Zafar, R. E. Jones, B. Jiang, B. White, V. Kaushik, and S. Gillespie, Appl. Phys. Lett. **73**, 3533 (1998).
[25] With permittivities of 300 (BST) and 7.3 (Al_2O_3) and a BST thickness of 250 nm a bias voltage of 1 V corresponds to an electric field of 40 kV/cm in BST without Al_2O_3, to 28 and 1165 kV/cm in BST and Al_2O_3 for 2.5 nm Al_2O_3 thickness, and to 15 and 622 kV/cm in BST and Al_2O_3 for 10 nm Al_2O_3 thickness.
[26] U. Ellerkmann, R. Liedtke, U. Böttger, and R. Waser, Appl. Phys. Lett. **85**, 4708 (2004).
[27] W.-K. Shih, E. X. Wang, S. Jallepalli, F. Leon, C. M. Maziar, and A. F. Tasch Jr., Solid-State Electron. **42**, 997 (1998).